

# Spin-orbit coupling in symmetric and mixed spin-symmetry

Ayaka Usui,<sup>1,2,3,\*</sup> Abel Rojo-Francàs,<sup>1,2</sup> James Schloss,<sup>4</sup> and Bruno Juliá-Díaz<sup>1,2</sup>

<sup>1</sup>*Departament de Física Quàntica i Astrofísica, Universitat de Barcelona, Martí i Franqués, 1, E08028 Barcelona, Spain*

<sup>2</sup>*Institut de Ciències del Cosmos (ICCUB), Universitat de Barcelona, Martí i Franqués, 1, E08028 Barcelona, Spain*

<sup>3</sup>*Grup d'Òptica, Departament de Física, Universitat Autònoma de Barcelona, 08193 Bellaterra, Spain*

<sup>4</sup>*Massachusetts Institute of Technology, Cambridge, MA, United States*

Synthetically spin-orbit coupling in cold atoms couples the pseudo-spin and spatial degrees of freedom, and therefore the inherent spin symmetry of the system plays an important role. In systems of two pseudo-spin degrees, two particles configure symmetric states and anti-symmetric states, but the spin symmetry can be mixed for more particles. We study the role of mixed spin symmetry in the presence of spin-orbit coupling and consider the system of three bosons with two hyper-fine states trapped in a harmonic potential. We investigate the ground state and the energy spectrum by implementing exact diagonalization. It is found that the interplay between spin-orbit coupling and repulsive interactions between anti-aligned pseudo-spins increases the population of the unaligned spin components in the ground state. The emergence of the mixed spin symmetric states compensates for the rise of the interaction energy. With the aligned interaction on, the avoided crossing between the ground state and the first excited state is observed only for small interaction, and this causes shape changes in the spin populations. Furthermore, we find that the pair correlation of the ground state shows similarly to that of Tonks-Girardeau gas even for relatively small contact interactions and such strong interaction feature is enhanced by the spin-orbit coupling.

## I. INTRODUCTION

Spin-orbit coupling (SOC) was originally discussed in the system of charged particles and, for instance, studied in the context of the spin Hall effect [1] or topological insulators states [2]. However, by using cold atomic systems it is possible to create synthetic SOC in neutral (pseudo) spin-1/2 bosons [3, 4], spin-1 Bose gases [5] and also in Fermi gases [6, 7]. In contrast to condensed matter systems, cold atoms can provide tunable and clean platforms and allow us to explore all possible states generated by SOC.

SOC in cold atoms is often discussed in the context of the mean-field regime, e.g. [8–10]. While the mean-field approximation has revealed interesting results, for example discovering the phase diagram [8], it imposes classical fields and ignores the quantum effects. To bridge single-particle physics and many-body physics in the SOC system, a mapping between the SOC cold atomic system and the Dicke model has been proposed [11]. However, the validity of the mapping is not obvious. The assumption imposed for the mapping is that all particles occupy the same real space state, which automatically leads to the pseudo-spin state spanned in only symmetric spin space. This assumption is commonly used for Bose gases with two internal degrees of freedom [12], however SOC couples pseudo-spin states and real space states and allows pseudo-spin states to get out of the symmetric spin space. It is not clear how even the lowest energy state is confined in symmetric spin space.

The spin symmetry of the ground state in the two-particle system with SOC has been investigated by per-

forming exact diagonalization [13]. Competition between SOC and contact interaction has been studied, and the emergence of anti-symmetric pseudo-spin states for strong interactions has been found. Despite using a bosonic system, anti-symmetric pseudo-spin states are preferable for the ground state. This work has also revealed the parameter regime where anti-symmetric pseudo-spin states or only symmetric pseudo-spin states are contained. However, these results cannot be extended to many-particle systems straightforwardly. One of the reasons is because two-pseudo-spin states have unique spin symmetry. Particles with two internal degrees of freedom are classified into symmetric and anti-symmetric pseudo-spin states, but the spin symmetry can be mixed in more-particle systems and anti-symmetry under all permutation of pseudo-spins no longer exist. It is unclear how the mixed spin symmetry affects the property of the ground state.

In this work, we investigate the role of mixed spin symmetry in the SOC system. To this end, we consider a three-particle system with two internal states as it is the smallest system that has mixed spin symmetry and focus on comparison with a two-particle system. We have built the Hamiltonian of three bosons with pseudo-spin-1/2 in the presence of SOC by considering second quantisation and computed the ground state. Our numerical results confirm the appearance of mixed symmetric pseudo-spin states in the ground state for strong interaction between anti-aligned pseudo-spins and reveal the parameter regime where it is observed. Furthermore, the emergence of the mixed spin symmetry states reduces the interaction energy. This is also seen in the two-particle system when the anti-symmetric pseudo-spin states emerge. This implies that the mixed spin symmetric state mimics the anti-symmetric pseudo-spin state to suppress the energy. In addition, we study the spatial structure of the ground

\* ayaka.usui@uab.cat

state by looking at the pair correlation and find that SOC assists contact interaction in inducing a strong interaction effect. Even for relatively small contact interaction, the pair correlation of the ground state has similarly to the strongly correlated Tonks-Girardeau gas. This is not observed in the two-particle system.

The structure of this paper is as follows. Section II explains the basis of our system. First, we introduce the Hamiltonian of our system in the first quantization representation and then transform it into the second quantization representation. This is necessary to implement exact diagonalization. Next, we explain the spin symmetry in pseudo-spin-1/2 systems and clarify the existence of non-symmetric pseudo-spin states, which are often ignored. Section III shows our numerical results of the ground state and the energy spectrum. We consider two cases, (i) repulsive interaction between anti-aligned pseudo-spins and (ii) repulsive interaction between aligned pseudo-spins. The conclusion is given in Sec. IV.

## II. FEW INTERACTING BOSONS WITH SOC

We present our formalism here. First, we introduce the Hamiltonian of our system in the first quantization basis and then rewrite it in the second quantization basis to induce the bosonic symmetry. This approach is often used to present the Hamiltonian of few particle systems, e.g. [14–16], and we refer interested readers to a detailed reference [17]. Second, we explain the spin symmetry of two spins and more spins respectively. While bosonic systems with two hyper-fine states are well studied, usually only pseudo-spin symmetric states are focused on, and the existence of anti-symmetry and mixed spin symmetry does not attract attention. We review the categories of spin symmetry before showing our numerical results.

### A. Hamiltonian in the first quantisation basis

We consider a few bosons trapped in a one-dimensional harmonic potential with two internal degrees of freedom in the presence of SOC. The Hamiltonian reads

$$\hat{H} = \hat{H}_0 + \hat{H}_{\text{int}}. \quad (1)$$

The single-particle Hamiltonian is given by

$$\hat{H}_0 = \sum_{j=1}^{N_p} \left( \frac{\hat{p}_j^2}{2m} + \frac{m\omega^2 \hat{x}_j^2}{2} + \frac{\hbar k}{m} \hat{p}_j \hat{\sigma}_z^{(j)} + \frac{\hbar\Omega}{2} \hat{\sigma}_x^{(j)} \right), \quad (2)$$

where the third term is the SOC term and describes coupling between real space and pseudo-spin space and the fourth term is coherent coupling between pseudo-spins. The SOC term gives positive momentum to down spins and negative momentum to up spins. Without either of these terms, the single-particle Hamiltonian can be diagonalised with the basis of  $\hat{\sigma}_z$  or  $\hat{\sigma}_x$ . The interaction

Hamiltonian can be decomposed into pseudo-spin basis as

$$\hat{H}_{\text{int}} = \hat{H}_{\downarrow\downarrow} + \hat{H}_{\downarrow\uparrow} + \hat{H}_{\uparrow\uparrow}. \quad (3)$$

Each of the components describes contact interaction and is given by

$$\hat{H}_{\downarrow\downarrow} = \sum_{i<j} g_{\downarrow\downarrow} \delta(x_i - x_j) |\downarrow\rangle_i |\downarrow\rangle_j \langle\downarrow|_i \langle\downarrow|_j, \quad (4)$$

$$\hat{H}_{\uparrow\uparrow} = \sum_{i<j} g_{\uparrow\uparrow} \delta(x_i - x_j) |\uparrow\rangle_i |\uparrow\rangle_j \langle\uparrow|_i \langle\uparrow|_j, \quad (5)$$

$$\hat{H}_{\downarrow\uparrow} = \sum_{i<j} g_{\downarrow\uparrow} \delta(x_i - x_j) \left( |\downarrow\rangle_i |\uparrow\rangle_j \langle\downarrow|_i \langle\uparrow|_j + |\uparrow\rangle_i |\downarrow\rangle_j \langle\uparrow|_i \langle\downarrow|_j \right). \quad (6)$$

### B. Hamiltonian in the second quantization basis

The above formalism is called the first quantization and describes distinguishable particles. To express indistinguishable particles simply, we implement the second quantization representation in a truncated space. Consider that  $N$  particles occupy  $N$  of first  $M$  eigenstates of the harmonic oscillator for down spins and up spins. Defining the creation and annihilation operators for the  $j$ th eigenstate as  $\hat{a}_j$  and  $\hat{a}_j^\dagger$ , the second quantised version of the single-particle part (2) is given by

$$\hat{H}_0 = \sum_{i,j=1}^{2M} \hat{a}_i^\dagger \hat{a}_j \epsilon_{i,j}, \quad (7)$$

where the indices  $i, j$  include the label of the eigenstates of the harmonic oscillator and the label of the pseudo-spin degrees. Specifically, we take numbers in  $[1, M]$  for the eigenstates for down spins and numbers in  $[M+1, 2M]$  for the eigenstates for up spins. The single-particle energy is represented as [15]

$$\begin{aligned} \epsilon_{i,j} = & \hbar\omega \left( n_x(i) + \frac{1}{2} \right) \delta_{i,j} + \frac{ik\xi}{\sqrt{2}} m_s(j) \delta_{m_s(i), m_s(j)} \\ & \times \left( \sqrt{n_x(j)+1} \delta_{n_x(i), n_x(j)+1} - \sqrt{n_x(j)} \delta_{n_x(i), n_x(j)-1} \right) \\ & + \frac{\hbar\Omega}{2} \delta_{m_s(i), -m_s(j)} \delta_{n_x(i), n_x(j)}, \end{aligned} \quad (8)$$

where  $\xi = \sqrt{\hbar/m\omega}$  is the trap length,  $n_x(j)$  represents the label of eigenstate of the harmonic oscillator, and  $m_s(j)$  represents the pseudo-spin state: down spins give  $m_s(j) = -1$ , and up spins give  $m_s(j) = 1$ . The interac-

tion part (3) is given by

$$\begin{aligned} \hat{H}_{\text{int}} = & \frac{1}{2} \sum_{i,j,k,l=1}^{2M} \hat{a}_i^\dagger \hat{a}_j^\dagger \hat{a}_k \hat{a}_l V_{i,j,k,l} \\ & \times \left( g_{\downarrow\downarrow} \delta_{m_s(i),-1} \delta_{m_s(j),-1} \delta_{m_s(k),-1} \delta_{m_s(l),-1} \right. \\ & + g_{\uparrow\uparrow} \delta_{m_s(i),1} \delta_{m_s(j),1} \delta_{m_s(k),1} \delta_{m_s(l),1} \\ & + g_{\downarrow\uparrow} (\delta_{m_s(i),1} \delta_{m_s(j),-1} \delta_{m_s(k),1} \delta_{m_s(l),-1} \\ & \left. + \delta_{m_s(i),-1} \delta_{m_s(j),1} \delta_{m_s(k),-1} \delta_{m_s(l),1}) \right), \quad (9) \end{aligned}$$

where

$$V_{i,j,k,l} = \int_{-\infty}^{\infty} dx \phi_{n_x(i)}(x) \phi_{n_x(j)}(x) \phi_{n_x(k)}(x) \phi_{n_x(l)}(x) \quad (10)$$

with  $\phi_n$  the  $n$ th eigenstate of harmonic oscillator. The above integral (10) can be solved analytically but is hard to compute for large indices as binomial coefficients appear. See Ref. [16] for an efficient calculation of it.

### C. Spin symmetry of bosons with two internal states

Here, we review the symmetry of pseudo-spin-1/2 systems, and let us start with two-particle states. Since we consider bosons, every state is symmetric under permutation. The considered system has the pseudo-spin degree and the spatial degree of freedom, and the pseudo-spin basis are classified into three symmetric pseudo-spin states,  $|\downarrow\downarrow\rangle$ ,  $(|\downarrow\uparrow\rangle + |\uparrow\downarrow\rangle)/\sqrt{2}$ ,  $|\uparrow\uparrow\rangle$  and one anti-symmetric pseudo-spin state  $(|\downarrow\uparrow\rangle - |\uparrow\downarrow\rangle)/\sqrt{2}$ . To satisfy the bosonic symmetry, the spatial states of symmetric pseudo-spin states are symmetric, i.e. even functions in the relative coordinate  $x_1 - x_2$ . Similarly, the spatial states of anti-symmetric pseudo-spin states are anti-symmetric, i.e. odd functions in the relative coordinate  $x_1 - x_2$ . Since the contact interaction occurs at a point and is described as the delta function  $\delta(x_1 - x_2)$ , the anti-symmetric spatial states do not feel the contact interaction.

By adding more particles to the system, the spin symmetry is mixed, and the anti-symmetry under all permutation does not exist anymore. Specifically, states of three bosons with pseudo-spin-1/2 can be constructed with the following symmetric spin basis,

$$\begin{aligned} |S_1\rangle &= |\downarrow\downarrow\downarrow\rangle \\ |S_2\rangle &= \frac{1}{\sqrt{3}} (|\downarrow\downarrow\uparrow\rangle + |\downarrow\uparrow\downarrow\rangle + |\uparrow\downarrow\downarrow\rangle) \\ |S_3\rangle &= \frac{1}{\sqrt{3}} (|\downarrow\uparrow\uparrow\rangle + |\uparrow\downarrow\uparrow\rangle + |\uparrow\uparrow\downarrow\rangle) \\ |S_4\rangle &= |\uparrow\uparrow\uparrow\rangle, \quad (11) \end{aligned}$$

and the following mixed spin symmetric basis,

$$\begin{aligned} |M_1\rangle &= \frac{-1}{\sqrt{6}} (|\downarrow\uparrow\uparrow\rangle + |\uparrow\downarrow\uparrow\rangle - 2|\uparrow\uparrow\downarrow\rangle) \\ |M_2\rangle &= \frac{1}{\sqrt{6}} (|\uparrow\downarrow\downarrow\rangle + |\downarrow\uparrow\downarrow\rangle - 2|\downarrow\downarrow\uparrow\rangle) \\ |M_3\rangle &= \frac{1}{\sqrt{2}} (|\uparrow\downarrow\uparrow\rangle - |\downarrow\uparrow\uparrow\rangle) \\ |M_4\rangle &= \frac{1}{\sqrt{2}} (|\uparrow\downarrow\downarrow\rangle - |\downarrow\uparrow\downarrow\rangle). \quad (12) \end{aligned}$$

For example, switching the first spin and the second spin in the pseudo-spin basis  $|M_1\rangle$  changes nothing (symmetric), but by switching the second spin and the third spin, the resultant state cannot be described with  $|M_1\rangle$  anymore. Therefore, these basis do not belong to symmetry or anti-symmetry but are called mixed symmetry. To satisfy symmetry under all permutation, the spatial states of the mixed spin symmetric states are neither symmetric nor anti-symmetric but formed such that the total state is symmetric.

When the spatial states and the pseudo-spin states are decoupled in systems of pseudo-spin-1/2 bosons, the pseudo-spin space is confined to the symmetric spin space. For instance, a pseudo-spin-1/2 BEC in a harmonic trap can be modelled with the collective spin operators, and the pseudo-spin Hamiltonian is expressed as  $\hat{H} = g\hat{S}_z^2$  [12]. The influence of the spatial state is included in the interaction strength  $g$ , and the strength  $g$  can be tuned by modifying the potential for example. However, SOC couples the spatial degree and the pseudo-spin degree, and the pseudo-spins can be non-symmetric. For instance, in the two-particle system, relative motion is induced by coupling between symmetric and anti-symmetric spin states (see Eq. (3) in Ref. [13]). Non-symmetric spin states play as an important role as symmetric spin states in the system with SOC.

## III. NUMERICAL RESULTS

We construct the Hamiltonians (7)(9) and diagonalize them in a truncated space numerically. In this work, we fix  $g_{\downarrow\downarrow} = g_{\uparrow\uparrow} = g$  to keep the symmetry between down and up spins. Moreover, to study competition between SOC and contact interaction, we turn on the anti-aligned pseudo-spin interaction  $g_{\downarrow\uparrow}$  or the aligned pseudo-spin interaction  $g$ . The study of the two particle system has shown that these two cases give clear different properties in the ground state [13]. We use the trap energy  $\hbar\omega$  as the energy unit and normalise the parameters with the trap energy  $\hbar\omega$  and the trap length  $\xi = \sqrt{\hbar/m\omega}$ , and display normalised parameters in all the figures. Also, we fix  $k\xi = 4$  and set the cutoff of the truncated space as  $M = 50$ . We discuss the justification of the cutoff  $M$  in Appendix A, and our numerical code can be viewed in Ref. [18].

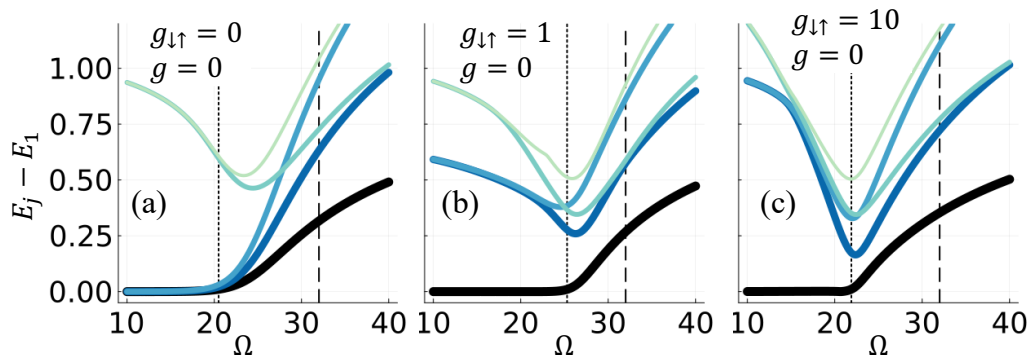


FIG. 1. Energy difference  $E_j - E_0$  between the first to fifth excited states and the ground state for (a) the non-interacting case, (b)  $g_{\downarrow\uparrow}/\hbar\omega\xi = 1$ , and (c)  $g_{\downarrow\uparrow}/\hbar\omega\xi = 10$ . The dashed line is the critical point  $\Omega_c^0/\omega = 2k^2\xi^2$  in free space, and the dotted line is when  $E_1$  and  $E_0$  start to deviate,  $(E_1 - E_0)/\hbar\omega > 0.01$ .

### A. Zero interactions ( $g = g_{\downarrow\uparrow} = 0$ )

It is known that SOC systems can have three different ground state phases [8]: the stripe phase, the magnetised phase, and the single minimum phase. In the stripe phase, the ground state is a superposition of positive and negative momenta and thus displays an interference pattern. In the magnetised phase, the ground state acquires positive or negative momentum, and in the single minimum phase the spectrum only possess a single minimum, leading to zero momentum usually. Without contact interactions, only the stripe phase and the single minimum phase exist, and at the critical point some degeneracies are resolved. In free space the critical point between these two phases is given analytically by  $\Omega_c^0/\omega = 2k^2\xi^2$ , and in trapped systems the density modulation modifies the critical value a lower value [19].

We plot the energy difference  $E_j - E_0$  between some excited states and the ground state for the noninteracting case ( $g = g_{\downarrow\uparrow} = 0$ ) for changing the coherent coupling strength  $\Omega$  and reconfirm that the degeneracy in the ground state is resolved off from  $\Omega_c^0$  (see the dashed line in Fig. 1(a)). Therefore, we define another critical point  $\Omega_c$  for the trap system as a point where the energy difference  $(E_1 - E_0)/\hbar\omega$  between the ground state and the first excited state is larger than  $10^{-2}$  (see the dotted line). In the absence of coherent coupling, the ground states are four-fold degenerate, and their pseudo-spin states are aligned pseudo-spins such as (i) three down-spins and (ii) three up-spins and upaligned pseudo-spins such as (iii) two up-spins and one down-spin (iv) one up-spin and two down-spins. Positive (negative) momentum is induced to down (up) spins due to SOC. The coherent coupling mixes these states, and in the strong coherent coupling limit an equally-weighted superposition of all pseudo-spin states obtains the lowest energy.

By adding contact interactions between pseudo-spins, the above four degenerate ground states (i-iv) obtain different energy. We discuss the ground state in the case of repulsive anti-aligned interactions ( $g_{\downarrow\uparrow} > 0$  and  $g = 0$ )

first and in the case of repulsive aligned interactions ( $g > 0$  and  $g_{\downarrow\uparrow} = 0$ ) later.

### B. Anti-aligned interactions ( $g_{\downarrow\uparrow} > 0$ and $g = 0$ )

We consider non-zero positive anti-aligned interaction  $g_{\downarrow\uparrow} > 0$ , i.e. when the unaligned pseudo-spin components suffer from repulsive interaction. As a result, in the absence of the coherent coupling only the aligned pseudo-spin states  $|\downarrow\downarrow\downarrow\rangle$ ,  $|\uparrow\uparrow\uparrow\rangle$  obtain the lowest energy. We have computed the energy spectrum for relatively weak interaction  $g_{\downarrow\uparrow}/\hbar\omega\xi = 1$  and for strong interaction  $g_{\downarrow\uparrow}/\hbar\omega\xi = 10$ . In the former (latter) case, the energy shift due to the contact interaction is less (more) than  $\hbar\omega$ . It is found that the degeneracy between the ground state and the first excited state is resolved at a different value of  $\Omega$  from the noninteracting case, and it depends on the interaction strength  $g_{\downarrow\uparrow}$  (see the dotted lines in Fig. 1(b,c)). Such deviation from the noninteracting case is also seen in the two-particle system but slightly smaller than in the three-particle system. This is because in the three-particle system the contact interaction energy is larger than in the two-particle system, and the maximum energy shift due to contact interaction is  $\hbar\omega$  for two particles and  $3\hbar\omega$  for three particles. For  $\Omega/\omega \simeq 40$ , the energy spectrum for different  $g_{\downarrow\uparrow}$  look similar to each other because the coherent coupling is so strong that the contact interaction contribution to the energy is negligible.

#### 1. Pseudo-spin population

We study the pseudo-spin component in the ground state. Here, we categorise the pseudo-spin population of the ground state into the aligned pseudo-spin components and the unaligned pseudo-spin components, i.e. the population  $p_{\text{aligned}}$  of  $|\downarrow\downarrow\downarrow\rangle$  and  $|\uparrow\uparrow\uparrow\rangle$  and the population  $p_{\text{unaligned}}$  of the rest of the pseudo-spin basis,

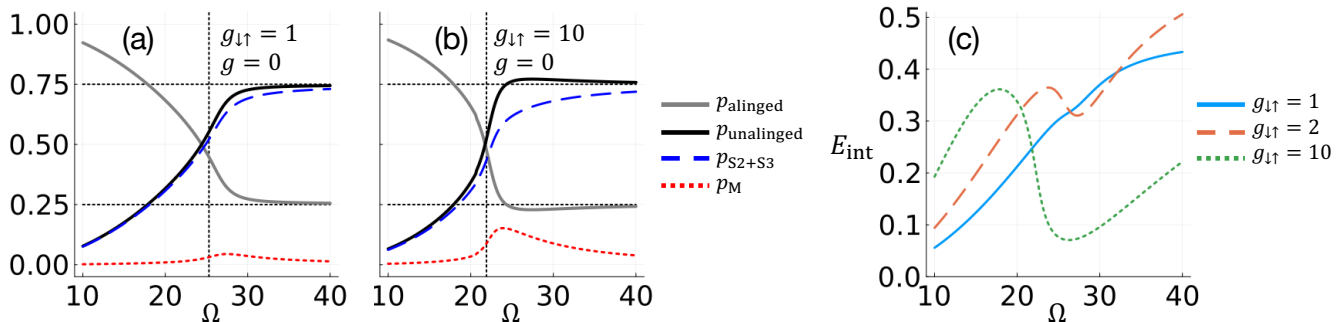


FIG. 2. (a,b) Pseudo-spin population  $p_{\text{aligned}}$ ,  $p_{\text{unaligned}}$  in the ground state for weak or strong contact interactions in the three-particle system. The dashed and dotted lines represent the population  $p_{S_2+S_3}$  of  $|S_2\rangle$  and  $|S_3\rangle$  and the population  $p_M$  of the mixed spin symmetry states, respectively. Note that  $p_{\text{unaligned}} = p_{S_2+S_3} + p_M$ . The dotted vertical lines represent  $\Omega_c$ . (c) Interaction energy for different  $g_{\downarrow\uparrow}$ .

therefore  $p_{\text{aligned}} + p_{\text{unaligned}} = 1$ . Note that the populations of  $|\downarrow\downarrow\downarrow\rangle$  and  $|\uparrow\uparrow\uparrow\rangle$  are the same due to the symmetry of the contact interactions we set ( $g_{\downarrow\downarrow} = g_{\uparrow\uparrow}$ ). We have plotted these pseudo-spin components  $p_{\text{aligned}}$ ,  $p_{\text{unaligned}}$  as a function of coherent coupling strength  $\Omega$  (see Fig. 2(a,b)). For weak coherent coupling  $\Omega$ , the aligned pseudo-spin population  $p_{\text{aligned}}$  is dominant because of repulsive anti-aligned interaction. By increasing  $\Omega$ , the unaligned pseudo-spin component  $p_{\text{unaligned}}$  also grows. Eventually, the population  $p_{\text{aligned}}$  is approaching  $3/4$  while  $p_{\text{unaligned}}$  is approaching  $1/4$ , because the lowest energy state in the limit  $\Omega \rightarrow \infty$  is

$$(|\uparrow\rangle - |\downarrow\rangle)^{\otimes 3} = |\uparrow\uparrow\uparrow\rangle - |\uparrow\uparrow\downarrow\rangle - |\uparrow\downarrow\uparrow\rangle - |\downarrow\uparrow\uparrow\rangle \\ + |\uparrow\downarrow\downarrow\rangle + |\downarrow\uparrow\downarrow\rangle + |\downarrow\downarrow\uparrow\rangle - |\downarrow\downarrow\downarrow\rangle.$$

In the intermediate regime, these populations  $p_{\text{aligned}}$ ,  $p_{\text{unaligned}}$  grow differently depending on  $g_{\downarrow\uparrow}$ . While for the weak interaction case (a) in Fig. 2 both populations increase monotonically, for the strong interaction case (b) in Fig. 2 the population  $p_{\text{aligned}}$  ( $p_{\text{unaligned}}$ ) reaches an extreme value and overcomes  $1/4$  ( $3/4$ ), i.e.  $p_{\text{aligned}}$  is concave, and  $p_{\text{unaligned}}$  is convex.

Furthermore, we have computed the population  $p_{M1}, p_{M2}, p_{M3}, p_{M4}$  of the mixed spin symmetric basis (12) (see the details of the calculation to Appendix B). Since these populations are the same due to our setting  $g_{\downarrow\downarrow} = g_{\uparrow\uparrow}$ , we have plotted the sum  $p_M = p_{M1} + p_{M2} + p_{M3} + p_{M4}$  (see the dotted lines in Fig. 2(a,b)). We have found that a large amount of the mixed spin symmetric states appear in the ground state for the strong interaction case (b) in Fig. 2. Considering  $p_{\text{unaligned}} = p_{S_2+S_3} + p_M$  with  $p_{S_2+S_3}$  the population of  $|S_2\rangle$  and  $|S_3\rangle$ , this leads to the non-monotonic growth of  $p_{\text{aligned}}$ ,  $p_{\text{unaligned}}$ . This is also seen in the two-particle system, and in that case it is originated from the emergence of the anti-symmetric pseudo-spin states [13]. The interaction energy increases for increasing the contact interaction strength in general, but the anti-symmetric pseudo-spin states do not feel contact interactions. Thus, the appearance of the anti-symmetric pseudo-spin states for

strong contact interactions suppresses the interaction energy. Therefore, it is a question whether the mixed spin symmetric states also reduce the interaction energy in the case we consider, and the answer is that they do. We have calculated the interaction energy  $E_{\text{int}} = \langle \hat{H}_{\text{int}} \rangle$  and plotted it as a function of  $\Omega$ , which displays a dent for strong interaction (see Fig. 2(c)). Finally, we have inspected the non-monotonic growth of  $p_{\text{unaligned}}$  for a wide range of interaction  $g_{\downarrow\uparrow}$  (see Fig. 3) and confirmed that the excess over  $3/4$  is larger for stronger  $g_{\downarrow\uparrow}$ .

## 2. Pair correlation

So far we have shown that the property of the ground state in the three particle system is similar to that in the two particle system regardless of the difference of the spin symmetry. The spatial structure of the ground state discussed in this section rather shows the opposite and reveals that the interplay between SOC and contact interactions brings a distinct feature from the two-particle

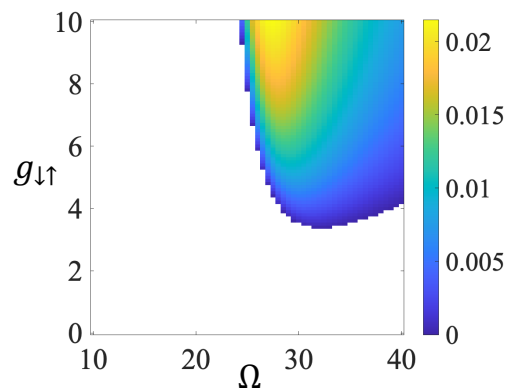


FIG. 3. Excess of  $p_{\text{unaligned}}$  over the population at the limit of  $\Omega \rightarrow \infty$  as function of  $\Omega/\omega$  and  $g_{\downarrow\uparrow}/\hbar\omega\xi$ , i.e.  $p_{\text{unaligned}} - 3/4$ . Negative values are not shown for clear presentation.

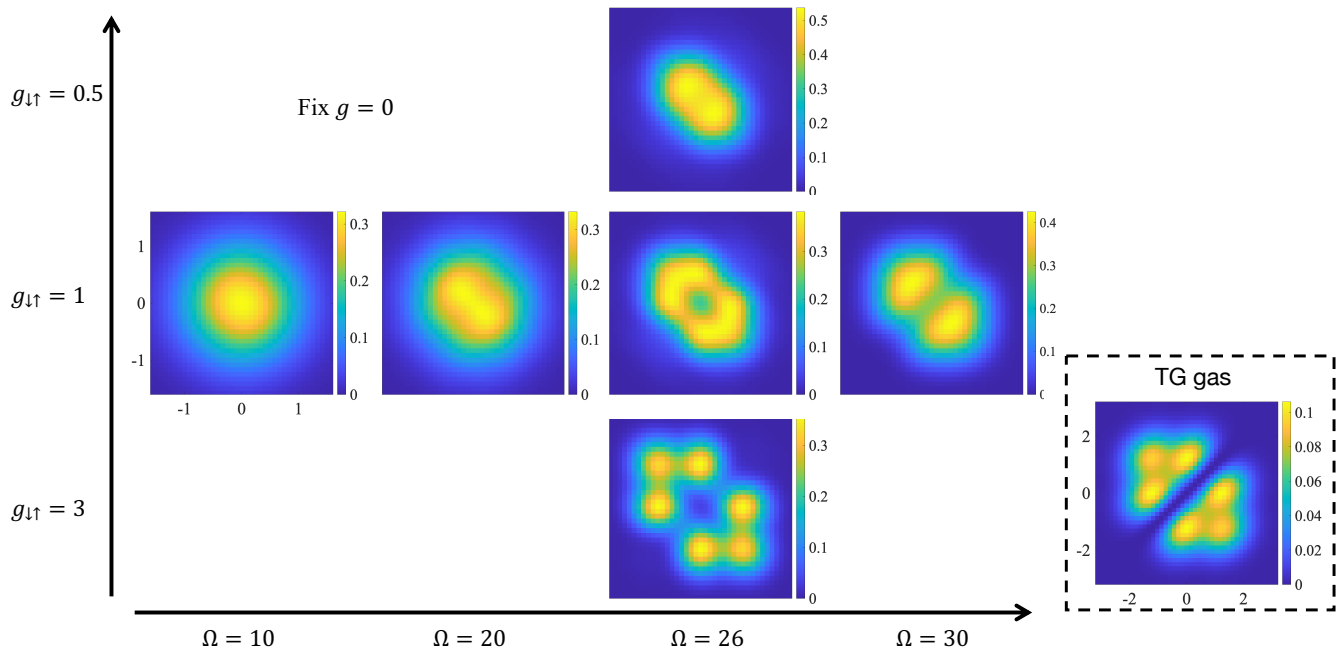


FIG. 4. Pair correlation of the ground state when changing  $g_{\uparrow\uparrow}$  and  $\Omega$  while fixing  $g = 0$ . The right panel displays the pair correlation of TG gas, and notice that the scale of the right panel is different from the other panels.

system.

The pair correlation of the ground state  $\Psi_{\text{GS}}(x_1, x_2, x_3)$  is defined as

$$\rho_2(x, y) = \int dx_3 |\Psi_{\text{GS}}(x, y, x_3)|^2, \quad (13)$$

where two of the spatial degrees are kept and the other is integrated out. In the second quantisation representation it is given by

$$\rho_2(x, y) = \frac{1}{N(N-1)} \sum_{i,j,p,q=1}^{2M} \langle \Psi_{\text{GS}} | \hat{a}_i^\dagger \hat{a}_p^\dagger \hat{a}_j \hat{a}_q | \Psi_{\text{GS}} \rangle \phi_i^*(x) \phi_p^*(y) \phi_j(x) \phi_q(y) \quad (14)$$

with  $\phi_i(x)$  the  $i$ th eigenstate of the harmonic oscillator and  $N = 3$  particle number [14]. The pair correlation of the free particle system is given by a two-dimensional Gaussian function,  $\rho_2(x, y) = |\phi_0(x)|^2 |\phi_0(y)|^2$ . In the limit of strong interactions  $g_{\uparrow\uparrow}, g \rightarrow \infty$ , the system corresponds to Tonks-Girardeau gas (TG) gas and behaves as (spinless) fermions [20–22], and particularly the density profile corresponds to that of the free fermions,  $|\Psi_{\text{TG}}(x_1, x_2, x_3)| = |\Psi_{\text{F}}(x_1, x_2, x_3)|$ . Therefore, the pair correlation in the limit can be calculated analytically by using the wavefunction of three free fermions trapped in the harmonic potential, given by

$$\Psi_{\text{F}}(x_1, x_2, x_3) = \frac{1}{\sqrt{3!}} \begin{vmatrix} \phi_0(x_1) & \phi_1(x_1) & \phi_2(x_1) \\ \phi_0(x_2) & \phi_1(x_2) & \phi_2(x_2) \\ \phi_0(x_3) & \phi_1(x_3) & \phi_2(x_3) \end{vmatrix}, \quad (15)$$

and is plotted for reference in the right panel in Fig. 4.

We study the pair correlations, and first let us focus on  $g_{\uparrow\uparrow}/\hbar\omega\xi = 1$  and change the coherent coupling strength  $\Omega$  (see the middle panels at  $g_{\uparrow\uparrow} = 1$  in Fig. 4). For relatively small coherent coupling  $\Omega/\omega = 10$ , the pair correlation is close to a Gaussian distribution, and the contact interaction affects the pseudo-spin populations but does not change the spatial structure of the ground state from the free particle case. By increasing the coherent coupling strength ( $\Omega/\omega = 20$ ), the shape is squished along  $x = y$ . At  $\Omega/\omega = 26$ , a dent emerges at the centre ( $x = y = 0$ ). For increasing  $\Omega$  more, a slit at  $x = y$  becomes deeper, and two bumps remain. This slit is originated solely from the contact interaction, and the pair correlation remains in the same shape even for larger  $\Omega$ . It is consistent to the pseudo-spin populations  $p_{\text{aligned}}$ ,  $p_{\text{unaligned}}$ , which reach plateau when  $\Omega/\omega \simeq 30$ .

To dig into the interplay between the contact interaction and the SOC, we fix the coherent coupling strength to  $\Omega/\omega = 26$  and change the contact interaction strength (see the panels at  $\Omega = 26$  in Fig. 4). By decreasing the contact interaction strength, the dent seen for  $g_{\uparrow\uparrow}/\hbar\omega\xi = 1$  becomes invisible. On the other hand, for increasing  $g$  the pair correlation shows three bumps in  $x > y$  and in  $x < y$ . This is a qualitatively similar feature to the TG gas other than the size of these bumps. It is interesting that such similarly to TG gas is seen even for relatively small interaction such as  $g_{\uparrow\uparrow}/\hbar\omega\xi = 3$ . For larger  $g_{\uparrow\uparrow}$ , the same structure remains. Also, it is worth noting that there is no interaction between the same pseudo-spins. In the two-particle system, the counterpart of the pair correlation is density distribution



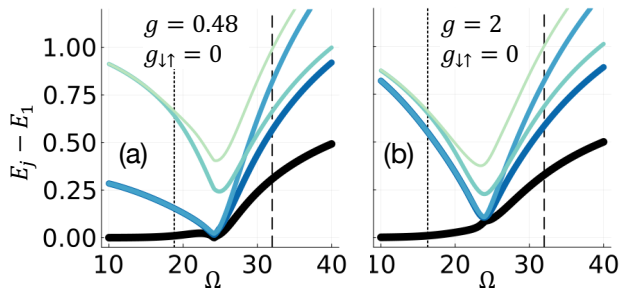


FIG. 5. Energy difference  $E_j - E_0$  between some excited states and the ground state for  $g/h\omega\xi = 0.48$  (a) and  $g/h\omega\xi = 2$  (b). The dashed line is the critical point  $\Omega_c^0/\omega = 2k^2\xi^2$  in free space, and the dotted line is when  $E_1$  and  $E_0$  start to deviate,  $(E_1 - E_0)/h\omega > 0.01$ .

$\rho_2(x_1, x_2) = |\Psi_{\text{GS}}(x_1, x_2)|^2$ , and it was investigated in our previous work [13]. However, such strong interaction feature enhanced by SOC is not observed.

### C. Aligned interaction ( $g > 0$ and $g_{\uparrow\downarrow} = 0$ )

Now we turn off anti-aligned interaction  $g_{\uparrow\downarrow} = 0$  and set non-zero aligned interaction strength  $g > 0$ . Any pseudo-spin configuration of three particle states has the aligned pseudo-spin components and is affected by the aligned interaction. For  $\Omega/\omega = 0$ , the two unaligned pseudo-spin states (the states (iii,iv) mentioned in Sec. III) obtain the lowest energy. For finite  $\Omega$ , the coherent coupling mixes those states and the two pseudo-spin aligned components  $|\downarrow\downarrow\downarrow\rangle, |\uparrow\uparrow\uparrow\rangle$ . In the limit  $\Omega \rightarrow \infty$ , the contact interaction contribution is not visible, and the ground state approaches that of no interactions.

Figure 5 reveals the energy difference  $E_j - E_0$  in the intermediate regime of  $\Omega$  for two different interaction strengths  $g/h\omega\xi = 0.48, 2$ . It is similar to the anti-aligned interaction case ( $g_{\uparrow\downarrow} > 0$ ) that the critical points  $\Omega_c$  vary in different interaction strengths. One different feature is that the avoided crossing between the ground state and the first excited states is seen for  $g/h\omega\xi = 0.48$  when  $\Omega/\omega \simeq 25$  but not for  $g/h\omega\xi = 2$ . This is caused by the interplay between the contact interaction and the coherent coupling that have attempt to shift energy in the opposite directions [23]. By increasing  $g$ , the excited states are pushed up, and accordingly the avoided crossing is shifted up and shades out eventually. The existence of this avoided crossing affects the pseudo-spin population as see below.

#### 1. Pseudo-spin population

As shown, in the anti-aligned interaction case ( $g_{\uparrow\downarrow} > 0$ ), the pseudo-spin populations  $p_{\text{aligned}}, p_{\text{unaligned}}$  become larger than the values in the limit  $\Omega \rightarrow \infty$  for larger

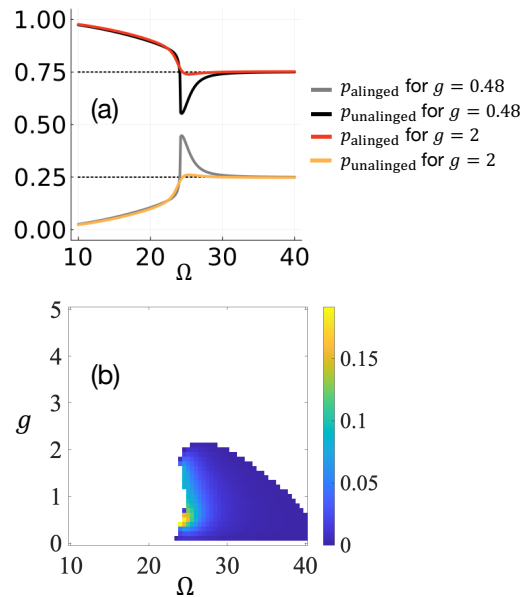


FIG. 6. (a) Pseudo-spin population  $p_{\text{aligned}}, p_{\text{unaligned}}$  in the ground state for  $g/h\omega\xi = 0.48$  and  $g/h\omega\xi = 2$ . (b) Excess of  $p_{\text{aligned}}$  over the population at the limit of  $\Omega \rightarrow \infty$  as function of  $\Omega/\omega$  and  $g/h\omega\xi$ , i.e.  $p_{\text{aligned}} - 1/4$ . Negative values are not shown for clear presentation.

interaction strength. In the aligned interaction case ( $g > 0$ ), the aligned pseudo-spin population  $p_{\text{aligned}}$  jumps up and the unaligned pseudo-spin population  $p_{\text{unaligned}}$  drops down for relatively weak interaction (see Fig. 6(a)). The emergence of this sharp change matches the appearance of the avoided crossing, and for large  $g$  these extreme values of  $p_{\text{aligned}}$  and  $p_{\text{unaligned}}$  disappear (see Fig. 6(b)). This is contrasted with the anti-aligned interaction case, where the pseudo-spin populations  $p_{\text{aligned}}$  and  $p_{\text{unaligned}}$  obtain the extreme values when  $\Omega = \Omega_c$ , i.e. when the degeneracy between the first excited state and the ground state is resolved. This non-monotonic behaviour survives only for small values of  $g$  compared to the anti-aligned interaction case because the emergence of aligned pseudo-spin states does not reduce the interaction energy. We note that such population jump has been also observed in the two-particle system [13].

#### 2. Pair correlation

We have computed the pair correlations for different  $g$  and  $\Omega$ . First, let us focus on  $g/h\omega\xi = 1$  and change  $\Omega$  (see the middle panels at  $g = 1$  in Fig. 7). Overall, the pair correlation behaves similar to the anti-aligned interaction case but is more sensitive to  $\Omega$ . Even for relatively small coupling, the pair correlation starts deviating from Gaussian distribution. For  $\Omega/\omega = 5$ , one bump appears at the centre ( $x = y = 0$ ), and for increasing  $\Omega$  four bumps come out. At  $\Omega/\omega = 26$ , where the populations  $p_{\text{aligned}}, p_{\text{unaligned}}$  approach the extreme values as shown

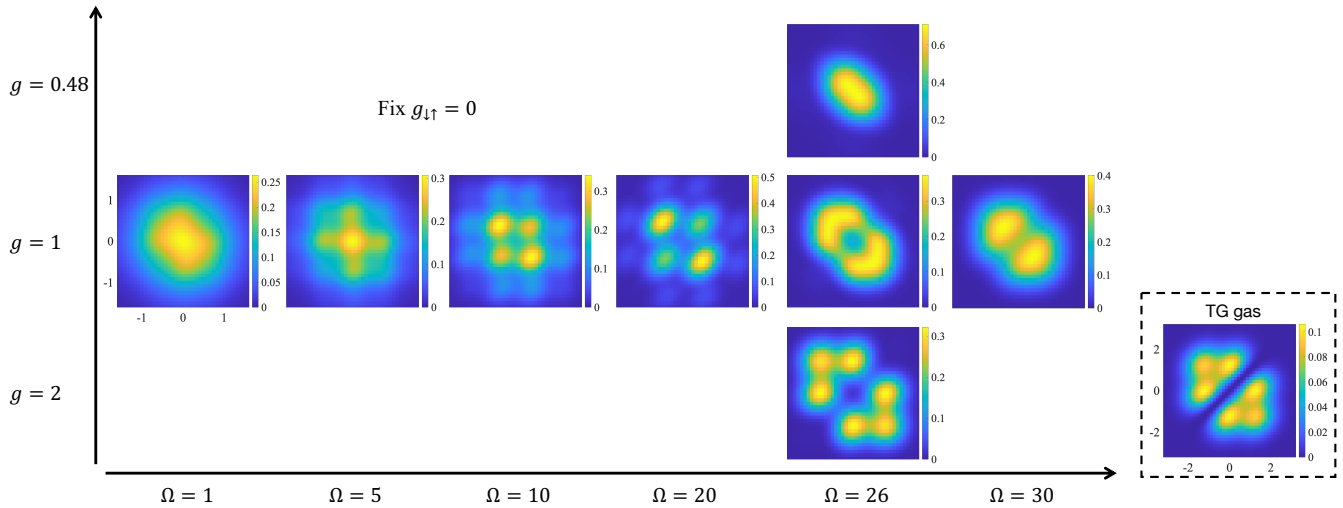


FIG. 7. Pair correlation of the ground state when changing for  $g$  and  $\Omega$  while fixing  $g_{\uparrow\uparrow} = 0$ . The right panel displays the pair correlation of TG gas, and notice that the scale of the right panel is different from the other panels.

in Fig. 5, a dent emerges at the centre. For increasing  $\Omega$  more, a slit at  $x = y$  caused by the contact interaction appears, and the effect of SOC vanishes.

Now we fix the coherent coupling strength to  $\Omega/\omega = 26$  and change the contact interaction strength to  $g/\hbar\omega\xi = 0.48, 2$ . For  $g/\hbar\omega\xi = 0.48$ , the dent at  $x = y = 0$  vanishes, and for  $g/\hbar\omega\xi = 2$  three bumps emerge in  $x > y$  and in  $x < y$  respectively, which is similar to the anti-aligned interaction case. The aligned interaction and the anti-aligned interaction give similar effects to the structure of the pair correlations even though they affect the energy spectrum and the pseudo-spin population differently.

#### IV. CONCLUSIONS

We have studied the system of three bosons trapped in a harmonic potential with two internal states in the presence of SOC and investigated the ground state and the energy spectrum by implementing exact diagonalization. Particularly, we focus on how the mixed spin symmetric states contribute to the ground state. We have found that the interplay between the anti-aligned contact interaction and SOC increases the population of the unaligned pseudo-spin components in the ground state. The emergence of the mixed spin symmetric states compensates for the rise of the interaction energy. This is similar to the two-particle system which has different spin symmetry. With the aligned interaction on, the avoided crossing between the ground state and the first excited state is observed only for small interaction, and this causes shape changes in the pseudo-spin populations. However, the emergence of aligned pseudo-spin states does not contribute to the reduction of the interaction energy, and therefore it decays out for strong interaction. Further-

more, we have found that the pair correlation of the ground state shows similarly to the TG gas even for relatively small contact interactions due to the interplay between contact interaction and SOC.

A question arises whether the same behaviour is seen in the more-particle systems. Our results cannot guarantee but implies that this would be the case for the anti-aligned interaction case. In the anti-aligned interaction case, the mixed spin symmetry affects the pseudo-spin populations, and the more-particle systems also have the same spin symmetry. The mixed spin symmetric states may act in the same way.

The mapping between Dicke model and the SOC system with contact interactions was proposed [11, 24, 25], assuming that the pseudo-spin space of the SOC system is only symmetric. However, as shown already, there is significant amount of mixed spin symmetric components even in the ground state for some parameter regime. Therefore, the mapping between these two models are limited.

In this work, we focus on the low energy states, but it is possible to study excited states and quench dynamics in a wide parameter range with our numerical method. As future work, it would be interesting to study transport via SOC [26] in the presence of strong interaction and utilise SOC, which gives different directions of momentum to different pseudo-spins, to create spatial entanglement [27–29].

#### V. ACKNOWLEDGEMENT

Discussions with Thomas Busch, Karol Gietka, Yongping Zhang, Peter Engels, Pere Mujal, and Ian B. Spielman are appreciated. We acknowledge funding from Grant No. PID2020-114626GB-I00 by



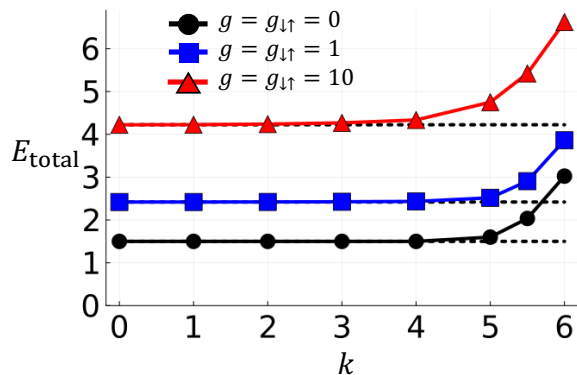


FIG. 8. Total energy for different interaction strengths  $g = g_{\uparrow\uparrow}$ , where  $\Omega = 0$  and  $M = 50$  are set. The dotted lines show the analytical results of the energy for  $k = 0$ .

MCIN/AEI/10.13039/5011 00011033 and “Unit of Excellence María de Maeztu 2020-2023” award to the Institute of Cosmos Sciences, Grant CEX2019-000918-M funded by MCIN/AEI/10.13039/501100011033. We also acknowledge financial support from the Generalitat de Catalunya (Grant 2021SGR01095). A.U acknowledges further support from the Agència Estatal de Investigació and the Ministerio de Ciencia e Innovación. A.R.-F. acknowledges funding from MIU through Grant No. FPU20/06174.

#### Appendix A: Justification of cut off $M$

In Sec. III, we set the SOC strength  $k\xi = 4$  and the cut off  $M = 50$ . Here, we show that the cut off  $M$  is large enough. As discussed in Sec. II B, the cut off  $M$  is the number of the eigenstates of the harmonic oscillator we take. The SOC couples these eigenstates such that the momentum of up spin or down spin is boosted. Although larger SOC needs larger  $M$ , the deviation from the results when  $k = 0$  is negligible if  $M$  is large enough.

Without coherent coupling  $\Omega$ , the Hamiltonian (1) can be diagonalised in the basis of  $\sigma_z$ , and the lowest energy can be obtained anaalytically and is the same as when

$k = 0$ . For instance, the kinetic term of the single particle Hamiltonian (2) can be written as  $\sum_{j=1}^N (p_j - \hbar k \sigma_z)^2 / 2m$ . The SOC acts as a moving frame, and the lowest energy does not change. Thus, by looking at the lowest energy for different  $k$ , we see whether the cut off  $M$  is large enough. Figure 8 shows the energy computed with  $M = 50$  as function of  $k$ . For large  $k$ , the energy obtained numerically deviates from the energy with  $k = 0$ . For strong interactions, the deviation is worse because strong interactions also couple highly excited eigenstates. For  $k\xi = 4$ , the error is small and at worst about 2.7% for  $g/\hbar\omega\xi = g/\hbar\omega\xi = 10$ , and we have taken  $k\xi = 4$  in the main text.

#### Appendix B: Population of mixed spin symmetry

In this work, we investigate the population of mixed spin symmetry and here explain how to compute it briefly. The mixed spin symmetry basis are described in the first quantization representation in Eq. (12). On the other hand, we adopt the second quantization representation for exact diagonalization (see Sec. II B). Therefore, we transform the second quantization representation of the Hamiltonians (7)(9) to the first quantization representation, i.e., label the particles and treat the system as distinguishable particles (see Fig. 9). This enables us to obtain the quantum number and the pseudo-spin state of each particles, i.e., have  $|n_1, \sigma_1; n_2, \sigma_2; n_3, \sigma_3\rangle$  for  $n_1, n_2, n_3 = 0, 1, \dots, M - 1$  and  $\sigma_1, \sigma_2, \sigma_3 = \downarrow, \uparrow$ . We transform the pseudo-spin basis using  $\downarrow, \uparrow$  to the classified pseudo-spin basis  $S_j, M_j$  by using the relations (11)(12). For more concrete details, see our code [18].

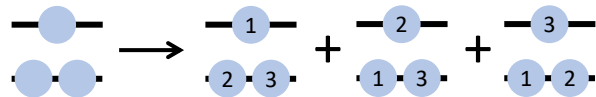


FIG. 9. Example of transforming the second quantization representation to the first quantization representation. The left hand shows a state of three indistinguishable particles, and the right hand shows superposition between three states of three distinguishable particles. These are summed up due to bosons.

[1] N. Nagaosa, J. Sinova, S. Onoda, A. H. MacDonald, and N. P. Ong, Anomalous hall effect, *Rev. Mod. Phys.* **82**, 1539 (2010).  
[2] M. Z. Hasan and C. L. Kane, Colloquium: Topological insulators, *Rev. Mod. Phys.* **82**, 3045 (2010).  
[3] Y. J. Lin, K. Jiménez-García, and I. B. Spielman, Spin-orbit-coupled bose-einstein condensates, *Nature* **471**, 83 (2011).  
[4] J.-Y. Zhang, S.-C. Ji, Z. Chen, L. Zhang, Z.-D. Du, B. Yan, G.-S. Pan, B. Zhao, Y.-J. Deng, H. Zhai, S. Chen, and J.-W. Pan, Collective dipole oscillations of a spin-orbit coupled bose-einstein condensate, *Phys. Rev. Lett.*

**109**, 115301 (2012).

[5] D. L. Campbell, R. M. Price, A. Putra, A. Valdés-Curiel, D. Trypogeorgos, and I. B. Spielman, Magnetic phases of spin-1 spin-orbit-coupled bose gases, *Nature Communications* **7**, 10897 (2016).  
[6] P. Wang, Z.-Q. Yu, Z. Fu, J. Miao, L. Huang, S. Chai, H. Zhai, and J. Zhang, Spin-orbit coupled degenerate fermi gases, *Phys. Rev. Lett.* **109**, 095301 (2012).  
[7] L. W. Cheuk, A. T. Sommer, Z. Hadzibabic, T. Yefsah, W. S. Bakr, and M. W. Zwierlein, Spin-injection spectroscopy of a spin-orbit coupled fermi gas, *Phys. Rev. Lett.* **109**, 095302 (2012).

- [8] Y. Li, L. P. Pitaevskii, and S. Stringari, Quantum tricriticality and phase transitions in spin-orbit coupled bose-einstein condensates, *Phys. Rev. Lett.* **108**, 225301 (2012).
- [9] Y. Zhang, L. Mao, and C. Zhang, Mean-field dynamics of spin-orbit coupled bose-einstein condensates, *Phys. Rev. Lett.* **108**, 035302 (2012).
- [10] Y. Zhang, M. E. Mossman, T. Busch, P. Engels, and C. Zhang, Properties of spin-orbit-coupled bose-einstein condensates, *Frontiers of Physics* **11**, 118103 (2016).
- [11] C. Hamner, C. Qu, Y. Zhang, J. Chang, M. Gong, C. Zhang, and P. Engels, Dicke-type phase transition in a spin-orbit-coupled bose-einstein condensate, *Nature Communications* **5**, 4023 (2014).
- [12] A. Sørensen, L. M. Duan, J. I. Cirac, and P. Zoller, Many-particle entanglement with bose-einstein condensates, *Nature* **409**, 63 (2001).
- [13] A. Usui, T. Fogarty, S. Campbell, S. A. Gardiner, and T. Busch, Spin-orbit coupling in the presence of strong atomic correlations, *New Journal of Physics* **22**, 013050 (2020).
- [14] P. Mujal, E. Sarlé, A. Polls, and B. Juliá-Díaz, Quantum correlations and degeneracy of identical bosons in a two-dimensional harmonic trap, *Phys. Rev. A* **96**, 043614 (2017).
- [15] P. Mujal, A. Polls, and B. Juliá-Díaz, Spin-orbit-coupled bosons interacting in a two-dimensional harmonic trap, *Phys. Rev. A* **101**, 043619 (2020).
- [16] A. Rojo-Francàs, A. Polls, and B. Juliá-Díaz, Static and dynamic properties of a few spin 1/2 interacting fermions trapped in a harmonic potential, *Mathematics* **8**, 10.3390/math8071196 (2020).
- [17] D. Raventós, T. Graß, M. Lewenstein, and B. Juliá-Díaz, Cold bosons in optical lattices: a tutorial for exact diagonalization, *Journal of Physics B: Atomic, Molecular and Optical Physics* **50**, 113001 (2017).
- [18] A. Usui, <https://github.com/ayaka-usui/SOCED> (2023).
- [19] C. Zhu, L. Dong, and H. Pu, Harmonically trapped atoms with spin-orbit coupling, *Journal of Physics B: Atomic, Molecular and Optical Physics* **49**, 145301 (2016).
- [20] L. Tonks, The complete equation of state of one, two and three-dimensional gases of hard elastic spheres, *Phys. Rev.* **50**, 955 (1936).
- [21] E. H. Lieb and W. Liniger, Exact analysis of an interacting bose gas. i. the general solution and the ground state, *Phys. Rev.* **130**, 1605 (1963).
- [22] M. A. García-March, B. Juliá-Díaz, G. E. Astrakharchik, T. Busch, J. Boronat, and A. Polls, Quantum correlations and spatial localization in one-dimensional ultracold bosonic mixtures, *New Journal of Physics* **16**, 103004 (2014).
- [23] Q. Guan, X. Y. Yin, S. E. Gharashi, and D. Blume, Energy spectrum of a harmonically trapped two-atom system with spin-orbit coupling, *Journal of Physics B: Atomic, Molecular and Optical Physics* **47**, 161001 (2014).
- [24] J. Lian, L. Yu, J. Q. Liang, G. Chen, and S. Jia, Orbit-induced spin squeezing in a spin-orbit coupled bose-einstein condensate, *Scientific Reports* **3**, 3166 (2013).
- [25] Y. Huang and Z.-D. Hu, Spin and field squeezing in a spin-orbit coupled bose-einstein condensate, *Scientific Reports* **5**, 8006 (2015).
- [26] X. Chen, R.-L. Jiang, J. Li, Y. Ban, and E. Y. Sherman, Inverse engineering for fast transport and spin control of spin-orbit-coupled bose-einstein condensates in moving harmonic traps, *Phys. Rev. A* **97**, 013631 (2018).
- [27] M. Fadel, T. Zibold, B. Décamps, and P. Treutlein, Spatial entanglement patterns and einstein-podolsky-rosen steering in bose-einstein condensates, *Science* **360**, 409 (2018), <https://www.science.org/doi/pdf/10.1126/science.aao1850>.
- [28] P. Kunkel, M. Prüfer, H. Strobel, D. Linne-mann, A. Frölian, T. Gasenzer, M. Gärttner, and M. K. Oberthaler, Spatially distributed multipartite entanglement enables epr steering of atomic clouds, *Science* **360**, 413 (2018), <https://www.science.org/doi/pdf/10.1126/science.aao2254>.
- [29] K. Lange, J. Peise, B. Lücke, I. Kruse, G. Vitagliano, I. Apellaniz, M. Kleinmann, G. Tóth, and C. Klempt, Entanglement between two spatially separated atomic modes, *Science* **360**, 416 (2018), <https://www.science.org/doi/pdf/10.1126/science.aao2035>.